Baffle Drop Structure Design Relationships

Article *in* Journal of Hydraulic Engineering · September 2013

DOI: 10.1061/(ASCE)HY.1943-7900.0000761

3 authors:

A. Jacob Odgaard
University of Iowa

Troy C Lyons
University of Iowa

Andrew J Craig
Iowa State University

Baffle-Drop Structure Design Relationships

A. Jacob Odgaard, F.ASCE[1]; Troy C. Lyons[2]; and Andrew J. Craig[3]

Abstract: A baffle-drop structure is a flow conveyance structure that can be used for transport of urban storm water down to underground storage tunnels. The water cascades down the structure from baffle to baffle and plunges into a pool at the bottom from where it is conveyed to the tunnel through an adit. The structure has been used successfully in a limited number of urban drainage schemes. However, its hydraulics and air entrainment characteristics are not fully understood. Using a series of laboratory experiments, an analysis has been tested and validated that may be used for design. The analysis provides a dimensionless relationship between key variables, including design discharge, shaft diameter, baffle spacing, and position of a vertical wall dividing the shaft in a dry and a wet portion. Using this relationship the shaft can be designed to maintain atmospheric pressure throughout its height with little or no air being entrained into the tunnel. **DOI: 10.1061/(ASCE)HY.1943-7900.0000761.** *© 2013 American Society of Civil Engineers.*

CE Database subject headings: Hydraulic structures; Drop structures; Stormwater management; Hydraulic models; Sewage; Air entrainment; Baffles; Structural design.

Author keywords: Hydraulic structures; Baffle-drop structure; Storm water management; Cascading flow; Hydraulic modeling; Combined sewage overflows; Air entrainment into underground tunnels; Energy dissipation in drop structure; Model to prototype scaling.

Introduction

One of the major challenges in urban storm water management is the handling of large discharges following extreme rainfall events. These challenges are exacerbated by global climate change, which appears to result in more frequent extreme events and consequent increased urban flooding. Many large cities are resorting to flood control strategies that include flow diversions and conveyance to underground storage tunnels through drop structures.

Different types of drop structure designs have been used over the years. They include the simple plunge type, in which the flow plunges into a pool or chamber for deaeration before being conveyed into the tunnel (U.S. Army Corps of Engineers 1997). In the so-called vortex type, the flow spirals down a shaft dissipating energy before plunging into the deaeration chamber (U.S. Army Corps of Engineers 1997). They also include the lesser-known baffle-drop shaft, in which the flow cascades down the shaft from one baffle to the next before entering the tunnel. A description of this type, including its history, was given recently by Margevicius et al. (2009).

Although the hydraulics of the plunge type and the vortex type structures are relatively well established (Falvey 1980; McKeogh and Ervine 1981; Jain and Kennedy 1983; Jain 1988; U.S. Army Corps of Engineers 1997; Yu and Lee 2009), the hydraulics of the baffle-drop structure is still being researched and documented. This paper presents an analysis for baffle-drop shafts that has been laboratory tested and used successfully for design of a limited number of prototype installations. The resulting design guidelines are presented in graphical form.

Baffle-Drop Shaft Features

The modern baffle-drop structure has a vertical partitioning wall that divides the structure into a dry side and a wet side. The baffles are positioned on the wet side as indicated in Fig. 1. The dry side is open and allows for surge mitigation, inspection, and maintenance. Inspection ports are located under each baffle as shown in Fig. 1. These ports also allow for air exchange between the dry and wet sides. By limiting the drop height between the baffles, baffle-drop structures keep flow velocities relatively low, limiting erosion potential and air entrainment. In addition, unlike vortex drop structures, baffle-drop structures do not require a specific approach-channel design to precondition the flow. The inflow to a baffle drop may be a standard sewer pipe, or several pipes entering at different elevations, without any modifications. One of the characteristic and distinguishing features of a baffle-drop shaft is that the flow cascades down the shaft from one baffle to the next with a plunge on each baffle. This succession of plunges is what distinguishes the baffle-drop structure from a straight-plunge shaft. As the flow plunges into a pool on each baffle, flow energy is dissipated. At the same time air is entrained. Because of the turbulence of the flow, air is also released. This study shows that there is no net inflow of air into or out of the shaft, and deaeration before the tunnel is not necessary. (Both the straight-plunge shaft and the vortex shaft require deaeration before the tunnel.) However, little data is available to determine how to size a baffle-drop structure for extreme events, and no data is available to determine its limiting flow capacity.

Analysis

The analysis of flow through the shaft is based on the following assumptions: (1) Flow is controlled on the baffle and is at critical

[1]Professor, Civil and Environmental Engineering, and Research Engineer, IIHR-Hydroscience and Engineering, Univ. of Iowa, Iowa City, IA 52242-1585 (corresponding author). E-mail: jacob-odgaard@uiowa.edu

[2]Director of Engineering Services, IIHR-Hydroscience and Engineering, Univ. of Iowa, Iowa City, IA 52242-1585.

[3]Hydraulic Engineer, IIHR-Hydroscience and Engineering, Univ. of Iowa, Iowa City, IA 52242-1585.

Note. This manuscript was submitted on May 10, 2012; approved on March 20, 2013; published online on March 22, 2013. Discussion period open until February 1, 2014; separate discussions must be submitted for individual papers. This paper is part of the ***Journal of Hydraulic Engineering***, Vol. 139, No. 9, September 1, 2013. © ASCE, ISSN 0733-9429/2013/9-995-1002/$25.00.

J. Hydraul. Eng. 2013.139:995-1002.

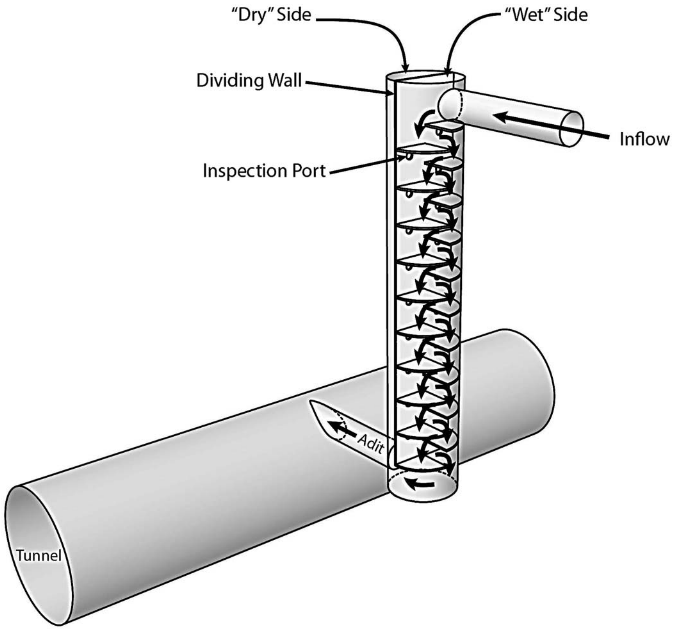

Fig. 1. Schematic of a baffle-drop structure

depth at the baffle edge; (2) flow exits each baffle in the form of a vented, rectangular jet; and (3) each jet impinges on the subsequent baffle in a plunge. Fig. 2 is a plan view of the drop shaft geometry showing the baffle and vertical dividing wall. Fig. 3 illustrates the typical flow pattern on the baffle shelves at design flow, using a photo from an actual baffle-drop shaft model as backdrop. Because of the curvature of the shaft wall and the nonuniformity of the flow as it approaches the baffle edge, the width of the ideal rectangular jet (effective width) is smaller than the actual width B of the baffle edge by a factor α_1. That is, effective width = $\alpha_1 B$. With the width of the rectangular jet equal to $\alpha_1 B$, critical depth is given by

$$y_c = \left[\frac{Q^2}{(\alpha_1 B)^2 g}\right]^{1/3} \tag{1}$$

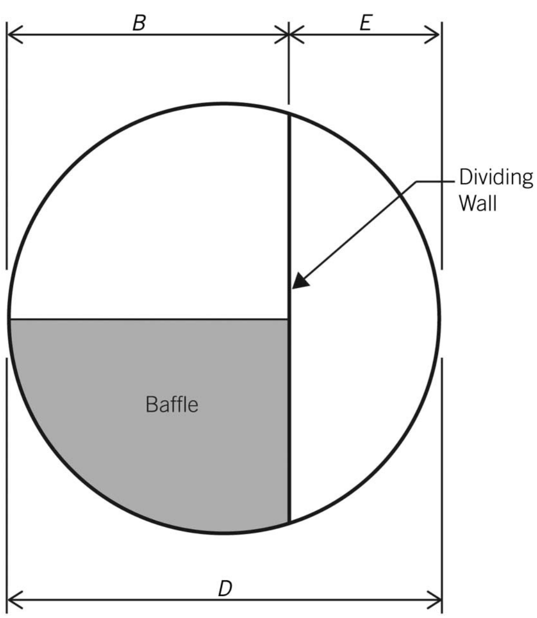

Fig. 2. Schematic top view of drop shaft showing baffle and vertical wall

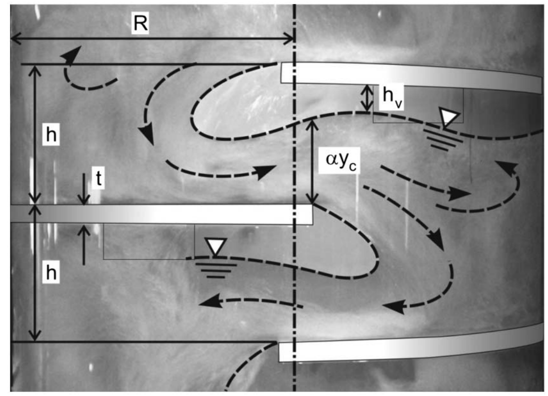

Fig. 3. Baffle flow schematic and related notation for a typical maximum discharge

where B = baffle width at the edge of the baffle; Q = design discharge; g = acceleration due to gravity; and α_1 = ratio of effective baffle width to actual baffle width at the edge of the baffle, a factor somewhat less than unity. At and near design flow, there is no or little drawdown at the overflow at the edge of the baffle (see Fig. 3). The design constraint is obtained by requiring the jet exiting a baffle to remain clear of (below) the opposite baffle with enough clearance to provide for full venting. By allowing for bulking, this constraint yields:

$$\alpha y_c \leq h - t - h_v \tag{2}$$

where α = bulking factor; h = vertical baffle separation; t = thickness of baffle shelf; and h_v = venting allowance (see Fig. 3). The bulking factor α is the factor by which depth on the baffle must be increased to account for entrained air. On spillways and chutes, this factor has been measured to range from 1.2 to 1.25. On baffles, due to the plunge from baffle to baffle, air entrainment is expected to be somewhat larger than on spillways. The design constraint then reads

$$\left(\frac{Q^2}{B^2 g}\right)^{1/3} \leq \beta(h - t - h_v) \tag{3}$$

or

$$\mathsf{F} \leq \beta\left(\frac{h-t}{B}\right) - \beta\frac{h_v}{B} \tag{4}$$

where $\beta = \alpha_1^{2/3}/\alpha$; and F is given by

$$\mathsf{F} = \left(\frac{Q^2}{B^5 g}\right)^{1/3} \tag{5}$$

The venting allowance h_v is the height of space between the jet surface and the baffle immediately above it (see Fig. 3) required for full venting of the nappe of the jet. The value of h_v must be large enough that air can pass freely back and forth between the nappe and the inspection ports at design flow without being blocked intermittently by spray from the water surface owing to turbulence. Intermittent blockage of the airflow would cause intermittent subatmospheric pressure at the nappe of the jet, which could potentially cause undesirable vibrations or load fluctuations on the baffle shelves. It follows that h_v is design specific; it depends on location and shape of the inspection ports. Results of this study show that to minimize h_v, the inspection ports should be located as close to the underside of the baffle as possible and away from

Fig. 4. View of the York model showing flow cascading down the baffle shelves on the wet side of the shaft; discharge $= 4\ \mathrm{m^3/s}$ (prototype) (image by authors)

the shaft wall, preferably half a baffle length or more toward the baffle edge. If they are located too close to the wall, the inspection ports become partially blocked at the large discharges owing to upwelling, i.e., water piled up as a result of horizontal jet momentum. To facilitate access and maintenance, the inspection ports are typically about 1 m tall and 3 m long (or 1-m-diameter circular holes) and located right underneath the baffles. This study showed that when they are located half a baffle length or more away from the shaft wall, required h_v is little dependent on location and shape of the inspection ports.

This study also showed that there is an upper limit to acceptable baffle spacing. If spacing is too large, rather than impinging on the subsequent baffle in a plunge, the jet hits the outside wall of the shaft before reaching the baffle. In this case, the flow becomes erratic and tends to set up a sweeping motion with little energy dissipation on the baffles. An estimate of the upper limit of acceptable baffle spacing is obtained by a simple jet-trajectory analysis. By assuming critical velocity v_c as the flow exits a baffle and a free-fall trajectory of the jet toward the subsequent baffle, the horizontal distance L from the edge of the baffle to the point of impingement is

$$L = v_c\sqrt{\frac{2\left(h+\frac{1}{2}\alpha y_c\right)}{g}} \tag{6}$$

Assuming that the length of a baffle is roughly half the shaft diameter D, the limitation on baffle spacing is obtained by requiring that L be well below the length of a baffle, i.e., well below half the shaft diameter. To make the jet impinge on the baffle over most of the effective width of the jet ($\alpha_1 B$), L must be less than approximately three-eighths the shaft diameter. Introducing Eqs. (1) and (5) and a critical velocity of $v_c = (Qg/\alpha_1 B)^{1/3}$, the requirement yields

$$2\left(\frac{h}{D}\right)\left(\frac{B}{D}\right)\mathsf{F} + \frac{1}{\beta}\left(\frac{B}{D}\right)^2\mathsf{F}^2 < 0.1 \tag{7}$$

With $\beta = 0.55$ (the approximate value found in this study) and $\mathsf{F} = 0.2$ (which is found in the experiments to be near the upper limit on F), Eq. (7) shows that if $B = 0.5D$, baffle spacing should be less than four-tenths the shaft diameter: $h < 0.4D$. If B is increased by 50% to $0.75D$, F is reduced to approximately 0.1 (assuming Q remains unchanged), and Eq. (7) shows that baffle spacing should be less than six-tenths the shaft diameter: $h < 0.6D$. Hence, for given Q, by increasing B by 50%, the upper limit on baffle spacing goes up by nearly the same percentage. In other words, by increasing B, the required number of baffles in a shaft may be reduced.

Calibration

The design relationship was tested and calibrated with data from a recent IIHR baffle-drop shaft project for the Regional Municipality of York, Canada (Lyons and Odgaard 2010). The shaft was 23 m tall with a diameter of $D = 12$ m and 3-m-diameter inlet and outlet pipes. The design discharge was $16.2\ \mathrm{m^3/s}$. It was modeled at a Froude scale ratio of 1:19.7. Fig. 4 shows the model as viewed toward the wet side. It shows the inlet at the top, the baffle shelves, and the outlet or adit to the tunnel at the bottom. (In the model, the tunnel was replaced by a sealed water and airflow control box.) The flow rate in Fig. 4 is $4\ \mathrm{m^3/s}$ (prototype). Fig. 5 shows a comparison of the flow pattern on the baffle shelves at design flow ($16.2\ \mathrm{m^3/s}$)

(a) (b) (c)

Fig. 5. Flow patterns at design discharge ($16.2\ \mathrm{m^3/s}$) with centrally located dividing wall and a baffle spacing of (a) 2.13; (b) 2.59; (c) 3.05 m (images by authors)

J. Hydraul. Eng. 2013.139:995-1002.

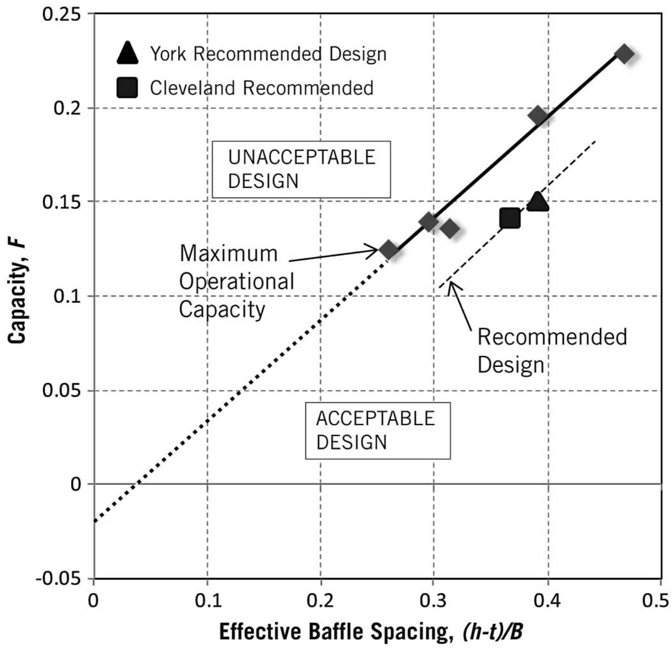

Fig. 6. Baffle-drop shaft design chart

as baffle spacing is varied from 2.13 to 2.59 to 3.05 m. In these cases, the dividing wall is centrally placed so $B = 1/2D$. For each baffle spacing, with the dividing wall centrally placed, tests were also conducted with the flow rate increased to maximum operational capacity, which is defined as the flow rate at which the venting of the jet started to become compromised. At maximum operational capacity, subatmospheric pressure along its surface caused the nappe of the jet to be drawn back and intermittently cling to the underside of the baffle. (At this limiting condition, water splashed through the 1-m inspection ports approximately 50% of the time as observed from the dry side of the dividing wall.) Maximum operational capacity was also determined for a shaft with the dividing wall shifted to the $2/3D$ and $3/4D$ positions; these tests were conducted with a baffle spacing of 2.59 m, only. In these tests, the lengths of the baffle edges were $2/3D$ and $3/4D$, respectively. Results are plotted in Fig. 6, which shows corresponding values of F and $(h-t)/B$ for the shaft at maximum operational capacity with the vertical wall between the wet and dry side in the center of the shaft ($B = R = 1/2D$) and at the $2/3D$ and $3/4D$ positions. The data defining the operational capacity relationship are from Lyons and Odgaard (2010). They are also listed in Table 1.

Fig. 6 shows the domain described by Eq. (5). It follows that a design will accommodate flow rates up to maximum operational capacity when design parameters (design discharge Q, baffle-edge B, and baffle spacing h) yield values of $[(h-t)/B, \mathsf{F}]$ below and to the right of the maximum operational capacity line.

The dimensions of the York shaft were originally proposed by the district to handle a design discharge of 16.2 m^3/s. For the 12-m diameter York shaft with a baffle edge B = shaft radius $R = 6$ m, the value of F is 0.15. The baffle spacing and thickness proposed by the district were $h = 2.59$ m and $t = 0.25$ m, respectively, yielding $(h-t)/B = 0.39$. As shown in Fig. 6, point $[(h-t)/B, \mathsf{F}] = (0.39, 0.15)$ plots below the threshold line and well into the acceptable design domain. The tests with this combination of variables showed acceptable flow pattern down the shaft with a plunge and visibly good energy dissipation on each baffle shelf. By proper gating of the outflow into the adit, as is explained later, no air was entrained into the outlet box (representing the tunnel).

When shaft discharge increases above the design discharge, the plotting point in Fig. 6 moves vertically upward. The plotting point reaches the line and the already indicated data point at the maximum operational capacity of 24 m^3/s.

Uncertainty

Obviously, there is uncertainty associated with the determination of maximum operational capacity. As mentioned, maximum operational capacity is defined as the flow rate at which the venting of the jet starts to become compromised. At this flow rate, the height of space between the jet surface and the overlying baffle, h_v, is so small that the free air passage between inspection port and nappe is blocked intermittently. This condition was determined by observations aided by video recordings. The results show a linear relationship between F and $(h-t)/B$ over the range covered by the experiments with a standard error of less than 10% in the value of $(h-t)/B$. The best-fit line through the data points (see Fig. 6) yield $\beta \approx 0.55$ and $h_v/B \approx 0.04$. For a baffle width of 6 m at the edge ($B = 6$ m), the minimum venting allowance is thus approximately 24 cm. The recommended relationship between F and $(h-t)/B$, the dashed line in Fig. 6, yields values of β and h_v/B of approximately 0.55 and 0.10, respectively. These values ensure adequate venting of the jet and provide a design with a reasonable margin of safety against undesirable, negative pressures on the underside of the baffles.

Flow rate was measured using a weigh-tank calibrated orifice meter accurate to ±2% of total flow. Flow meter pressure differentials were measured with a precision two-tube manometer accurate to ±0.15 mm. The uncertainty on F was less than 2%.

Validation

One data point in Fig. 6 is from IIHR's baffle-drop shaft project for the Ohio Regional Sewer District (Lyons et al. 2007, Test

Table 1. Experimental Values Used in the Design Chart

Test number	Flow rate $Q(m^3/s)$	Dividing wall position	Baffle edge B (m)	Baffle spacing h (m)	Baffle thickness t (m)	Effective baffle spacing $(h-t)/B$	Capacity F
1	16.2	$1/2D$	6.0	2.59	0.25	0.390	0.151
2[a]	13.8	$1/2D$	6.0	2.13	0.25	0.313	0.136
3[a]	24.0	$1/2D$	6.0	2.59	0.25	0.390	0.196
4[a]	30.5	$1/2D$	6.0	3.05	0.25	0.467	0.230
5[a]	30.1	$2/3D$	8.0	2.59	0.25	0.293	0.141
6[a]	33.7	$3/4D$	9.0	2.59	0.25	0.260	0.125
7	4.84	$1/2D$	3.8	1.68	0.30	0.363	0.144

[a]Test for determining maximum operational capacity.

J. Hydraul. Eng. 2013.139:995-1002.

No. 7 in Table 1, "Cleveland Recommended"; Margevicius et al. 2009). The Ohio baffle-drop shaft was 45.7 m tall with a diameter of 7.62 m and was modeled at a Froude scale ratio of 1:12.5. The design discharge was 4.84 m^3/s and baffle spacing was 1.68 m. A photo of this model is presented in Margevicius et al. (2009). The Ohio data point in Fig. 6 is for the final recommended design, which was tested before the formulation and calibration of the aforementioned analysis. As shown, the data point plots within the acceptable design domain. In an attempt to explore the feasibility of a larger baffle spacing, some of the baffles were removed to create 5.03-m baffle spacing in the upper portion of the shaft. This spacing was determined to be too large for a 7.62-m-diameter shaft, creating undesirable flow patterns on the baffle shelves. Instead of plunging onto the baffle shelf into a pool of water, the jet first impacted the outer wall of the shaft and was then directed forcefully onto the surface of the baffle shelf near the wall, thus eliminating the plunge pool and resulting in increased velocities and reduced energy dissipation. This resulted in considerably more splash, spray, and unsteadiness of the flow. This observation is in agreement with the previous analysis which shows that a plunge is assured only when $h < 0.63D$, i.e., when the baffle spacing is less than 4.8 m.

The analysis, based on five unique geometries, plus the York and Cleveland final (recommended) designs, establishes design relationships that provide a strong basis for application to alternative designs. For example, would reducing the York shaft diameter from 12 to 10 m while maintaining other variables unchanged keep the plotting point in the acceptable design domain? Using $B = R = 5.0$ m instead of 6.0 m, values of F and $(h - t)/B$ are 0.20 and 0.47, respectively. That is, the plotting point is still within the acceptable domain.

Recommended Design Relationship

The York final design may be used as a guide for other baffle-drop shaft projects. Scaling to other design discharges is straightforward because the design relationship is dimensionless, and plotting points only have to be at or near the dashed line in Fig. 6

$$\mathsf{F} = \beta\left(\frac{h-t}{B}\right) - \beta\frac{h_v}{B} \tag{8}$$

where $\beta = 0.55$ and $h_v/B = 0.1$. By reintroducing the design variables, the equation reads

$$\frac{h - t - h_v}{B} = \frac{1}{\beta}\left(\frac{Q^2}{B^5 g}\right)^{1/3} \tag{9}$$

or, for a relationship between B and Q,

$$B = \frac{Q}{\beta^{3/2}(h - t - h_v)^{3/2} g^{1/2}} \tag{10}$$

Although the York tests showed good performance for baffle-edge widths within the range $0.5D \le B \le 0.75D$, the final design was with $B = 0.5D$. Taking $B = 0.5D$ and using the optimum ratio between $(h - t)$ and B of 0.39 observed in the York tests and the corresponding venting allowance h_v/B of 0.1, Eq. (9) yields, with $\beta = 0.55$,

$$D = \frac{6.0}{g^{1/5}} Q^{2/5} \tag{11}$$

This equation may be used as a guide for the selection of shaft diameter given the design discharge and noting that the guide is valid only for effective baffle spacing of $(h - t)/B = 0.39$ and venting allowance of $h_v/B = 0.1$.

For comparison, Jain and Kennedy's (1983) and Yu and Lee's (2009) recommendation for a tangential vortex drop shaft is

$$D = \frac{k}{g^{1/5}} Q^{2/5} \tag{12}$$

where $k = 1.0 - 1.3$ (Yu and Lee 2009). For design, Yu and Lee (2009) recommends $k = 1.2$. Hence, a baffle-drop shaft with centered dividing wall requires a diameter that is approximately five times larger than that of a vortex drop shaft.

To demonstrate the application of Fig. 6, assume that a baffle-drop shaft is to convey a design discharge of 20 m^3/s. For a shaft with a centered dividing wall, Eq. (11) yields a required diameter of $D = 12.6$ m. Such a shaft, with $B = D/2 = 6.3$ m, has an F value of 0.16. Fig. 6 yields a recommended effective baffle spacing of $(h - t)/B = 0.4$. If baffle thickness is 0.25 m, the design will require a baffle spacing of $h = 2.77$ m or higher but less than 6.3 m. If the dividing wall is offset to the $3/4D$ position, the required shaft diameter is smaller. Assuming baffle spacing and thickness of 2.77 m and 0.25 m, respectively, and 60 cm venting allowance, Eq. (10) yields $B = 5.88$ m $= 0.75D$, i.e., $D = 7.85$ m. The plotting point for this latter design is $[(h - t)/B, \mathsf{F}] = (0.44, 0.18)$.

Airflows

One of the unique characteristics of a baffle-drop shaft is containment of airflows. In the Ohio and York shaft tests, to visualize airflows, fog was pumped through a lid on top of the shaft into the dry side. The entire shaft quickly filled with fog. Air was drawn through the inspection ports into the wet side and entrained into the bubbly flow on the baffle shelves. The fog quickly distributed downward, filling the entire shaft. Slow moving air currents were observed to move up and down on the dry side; however, none were observed that showed air entering or leaving the shaft through the lid on top for any of the flows tested. Some air may have been dragged into the shaft through the inflow pipes, but with the outlet surcharged at design flow, the amount would have been limited. The air remained at or near atmospheric pressure throughout the shaft.

The inspection ports seem to play an important role in maintaining constant air volume in the shaft. Without the flows through the ports being two-way flows, constant air volume would not be possible. Margevicius et al. (2009) suggest that the ports are "crucial to the longevity of the structure due to the assurance of atmospheric pressures throughout the height of the shaft." They suggest that one of the probable causes for baffle-drop shaft failure in the past has been subatmospheric pressures developing below the baffle shelves at high flows, causing vibration, fatigue, and ultimately, structural failure of the shelves.

The outlet size and location is also an important consideration in the airflow balance. To maintain this balance, air must be prevented from escaping into the tunnel at flows near and at design flow. The aforementioned tests have demonstrated that this is indeed possible when the shaft is adequately surcharged relative to the adit. To insure adequate surcharge for a range of flows at and near the design discharge, the adit flow must be inlet controlled. At inlet control, the relationship between surcharge and adit-inlet area A is the orifice equation

$$Q = C_d A\sqrt{2g\left(H - \frac{d}{2}\right)} \tag{13}$$

J. Hydraul. Eng. 2013.139:995-1002.

where C_d = discharge coefficient; d = adit-inlet diameter; and H = height of shaft-water surface elevation above adit-inlet invert. In the Ohio shaft, the adit inlet was sharp-edged with the invert at the same elevation as the bottom of the shaft, and the discharge coefficient was measured to be $C_d = 0.68$. In the York shaft, the inlet consisted of two vertical, rectangular gates separated by a strut, and the discharge coefficient was measured to be $C_d = 0.49$. Obviously, care must be taken that the effect of the inlet configuration on the discharge coefficient is fully understood in the design phase. In addition to the surcharge, the orientation of the adit inlet affects air entrainment into the tunnel. Air bubbles entrained with the jet from the lowest baffle must have sufficient time to rise to the surface and be released in the shaft rather than in the adit or in the tunnel. To provide the most time possible for air release within the shaft, the adit inlet should be placed at the bottom off the dry side of the shaft in the wall opposite the dividing wall away from the immediate vicinity of the bubbly flow created by the plunging jet. This is where the tests clearly demonstrated how the succession of plunges on the upper shelves helps dissipate flow energy and allows the nappe from the lowest baffle to plunge into the bottom pool at a slow enough velocity that the bubbles could easily rise to the surface before being entrained into the adit. This feature is, of course, most critical at or near design discharge and at or near tunnel-full condition, in which entrained air could potentially create air pockets along the tunnel crown.

For comparison, in the York test series, one series was conducted with baffles and dividing wall removed, i.e., the flow entered the shaft in a straight plunge. Inlet and outlet conditions remained unchanged. At design flow, the straight plunge caused considerable flow instability in the pool and a high rate of air entrainment. The air entrainment rate into the tunnel was measured to be approximately 49 m^3/min; this value is to be compared with a maximum of 9 m^3/min measured under similar conditions with baffles and dividing wall in place. (The straight plunge entrained considerably more than 49 m^3/min, but a significant amount of air escaped through the top lid of the shaft.)

Airflow Scaling

Froude scale models underestimate air entrainment and transport rates because the model Weber number is smaller than the prototype Weber number. Little is known about how much air entrainment and transport is underestimated. Ervine and Kolkman's (1980) study of air entrainment caused by a plunging drop shaft flow suggests that Froude scaling underestimates the air entrainment rate by a factor between 2 and 4. In their study of vortex flow drop structures for the Milwaukee Metropolitan Sewerage District, Jain and Kennedy (1983) obtained an estimate by comparing airflow rates in two models of different scales, a small-scale model and a large-scale model. The large-scale model was 2.3 times larger than the small-scale model. Their results suggest that airflow rates that are scaled according to Froude's law must be multiplied by an additional scaling factor equal to the prototype to model ratio raised to a power of 0.34. If this finding can be applied to a prototype that is 12.5 times larger, as in the Ohio study, and 19.7 times larger, as in the York study, then Froude-scaled airflow rates in these studies would have to be multiplied by an additional factor of 2.4 and 2.8, respectively. Considering that the Jain and Kennedy (1983) scaling relationship is based on scaling from one laboratory model to another that is only 2.3 times larger, using it for scaling from a model to a prototype that is 12.5 times or more larger than the model may be subject to considerable uncertainty.

Application

The design relationship and graph were used for recommending dimensions of drop shafts for the Fall Creek/White River Tunnel System for the City of Indianapolis and for selecting one of the shafts for model testing (Lyons et al. 2011). Six drop structures were considered along the White River leg, and 12 along the Fall Creek leg. Drop structure depths from ground level to adit invert range from approximately 60 to 73 m and design flow range from 1.7 to 12.8 m^3/s. A minimum space constraint was imposed on the dry side of the dividing wall to allow for personnel access with a two-person man cage. The dimensions of the 18 shafts were developed by selecting a central data point in Fig. 6, given by $(h-t)/B = 0.44$ and $[Q^2/(B^5 g)]^{1/3} = 0.163$. These dimensionless values were used to calculate corresponding values of Q and B subject to the constraints on dry space (a 0.91×1.52-m cage with 30 cm of clearance around it), a baffle thickness of 0.20 m, a venting allowance of 0.4 m, and allowance for construction equipment. Over the range of design discharges from 1.7 to 12.8 m^3/s, shaft diameters were calculated to vary from 5.18 to 7.30 m, baffle spacing to vary from 1.41 to 2.40 m, and baffle-edge length B to vary from 2.33 to 5.24 m.

The laboratory model was designed by fixing the model shaft diameter to 0.61 m (2 ft) and adjusting the scale ratio of each individual drop shaft based on the recommended prototype diameter. The 0.61-m-diameter model was selected to represent the drop shaft with a design discharge in the middle of the range of design discharges for the 18 structures: 8.10 m^3/s. Because of the aforementioned design constraints, the scale ratio of baffle-edge length for the other 17 structures was slightly off from that of their diameter. For the 18 drop structures, the scale ratios varied from 1:8.505 to 1:11.973. Fig. 7(a) shows a plot of corresponding values of $(h-t)/B$ and F for the 18 designs that the model represented. As shown, all but one of the 18 shafts could be modeled with a single geometry in the laboratory without significant deviation from the recommended design line. The 8.10-m^3/s design is represented by the point located right on the recommended design line. The outlier in the plot is for the shaft that requires a large diameter to provide construction access but has a relatively small design discharge.

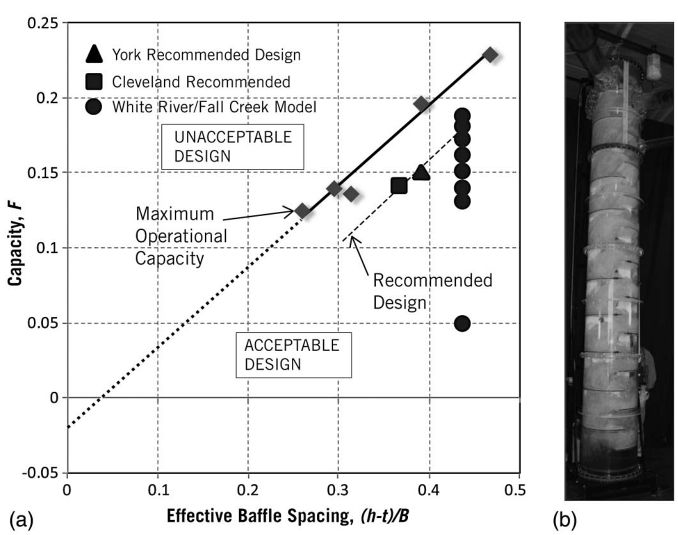

Fig. 7. Drop shaft modeling for the Fall Creek/White River Tunnel System: (a) plotting points (dots) for the 18 drop shafts represented by the model; (b) photograph of the model (image by authors)

J. Hydraul. Eng. 2013.139:995-1002.

A photograph of the completed model is shown in Fig. 7(b). As mentioned, the design flow rate for the drop structure that was modeled was 8.10 m^3/s, which represented the midrange of the design flow rates for the 18 drop structures included in the Fall Creek/White River Tunnel System project. The modeled drop structure height was approximately 47.2 m. This corresponded to 4.54 m from the centerline of the upper inlet pipe to the floor of the drop structure. A higher/taller drop structure model was not necessary because it was shown in previous studies that baffle shelf hydraulics are independent of drop height after 3 or 4 baffles and therefore truncating the actual height to some extent is considered acceptable. The modeled shaft diameter was 6.40 m. The large inlet pipes were 2.41 m in diameter. The lower inlet pipe was 1.22 m in diameter at the adjusted model scale of 1:8.93 for modeling the largest of the drop structures. The adit was 2.67 m in diameter. The top section of the model could rotate 180 degrees to accommodate and test various inlet configurations.

The tests confirmed that a shaft designed according to the guidelines presented in Fig. 6 provides acceptable hydraulics down the shaft. The tests were used to also check that elevation and orientation of inflow pipes were not critical to the hydraulic performance of the baffles; air entrainment rate into the tunnel was low and controllable, notably by submerging the adit outlet (by raising tunnel water levels); and solids deposition is minimal as a result of the relatively high intensity of the turbulence both on the shelves and at the base of the shaft. Initially, the tests were conducted with a positive baffle overlap, meaning the baffles extended past the centerline of the shaft and overhung the adjacent baffles. Generally, a small overlap is recommended to keep water and debris from falling unimpeded between baffles to the bottom of the shaft during extreme flows. The initial geometry of the model was designed with a positive total baffle overlap of 0.46 m for each baffle. This means each baffle overlapped the centerline of the drop structure by 0.23 m. Although acceptable, the flow from baffle to baffle was shown to exhibit some unsteadiness, particularly at low flows. The flow could be described as spiraling down the wet side creating deep portions of flow near the outside of one baffle and shallow flow on the outside of the next. This depth nonuniformity seemed to be attributable to the jet impinging on the baffles too close to the outer wall of the shaft as a result of the overlap. Consequently, tests were conducted with some of the baffles shortened: some with zero overlap and others with minus 0.53 m overlap. Flow over the shortened baffles improved. The zero overlap baffles seemed to result in the most uniform flow over the baffles and was the recommended solution. Finally, the shaft's maximum operational capacity was measured to be 12.8 m^3/s. With this flow rate, the value of F is 0.22, which, together with the structure's $(h-t)/B$ value of 0.44 yields a plotting point right on the maximum operational capacity line in Fig. 7 (or Fig. 6).

Conclusions

The key variables used in this study for describing the design-flow condition in a baffle-drop shaft are design discharge, shaft diameter, baffle spacing, and location of the vertical dividing wall. Assuming that the design condition is one in which the design flow cascades down the shaft with a plunge (rather than sweep) on each baffle shelf and critical flow at each baffle edge, these variables form two dimensionless quantities that are uniquely related: Capacity F and effective baffle spacing $(h-t)/B$. The relationship has been calibrated and validated in three laboratory test series. These test series covered the following ranges of the dimensionless quantities: $0.12 < \mathsf{F} < 0.23$ and $0.26 < (h-t)/B < 0.47$, and have resulted in the following suggested (iterative) design steps:

1. Use Eq. (11) to obtain first estimate of shaft diameter, D; note that Eq. (11) is based on a baffle edge width of $B = D/2$, which implies that dry-space dimension E is also $D/2$.
2. If the dry-space requirement E is less than $D/2$, select a new (larger) value of B if desired: $B = D - E$.
3. Select baffle thickness, t.
4. Calculate F and enter Fig. 6 to obtain baffle spacing, h.
5. Adjust h to accommodate vertical space limitations and locate inflow and outflow pipes.
6. With the new value of h, get a new value of B from Eq. (10) and a new shaft diameter, $D = B + E$.
7. With the new value of B, check [Eq. (7)] that vertical baffle spacing is acceptable. If not acceptable, adjust h and repeat Steps 6 and 7.
8. Given D and Q, size adit and adit gates as necessary [Eq. (13)] to provide adequate surcharge at and near design discharge; and make sure the adit is inlet controlled.
9. Orient the adit or shaft so that the adit alignment is perpendicular to the dividing wall and as close to the bottom of the shaft as possible.
10. Place the lower edge of the dividing wall sufficiently low that air entrained from the plunge from the lowest baffle rises to the water surface on the wet side of the wall. In the tests, the lower edge was at or near the elevation of the lowest baffle located approximately one to one-and-a-half baffle spacing above the bottom of the shaft. If necessary, extend a portion of the dividing wall to the bottom of the shaft (as was done in the Indianapolis shaft).

One of the major advantages of a baffle-drop structure over the straight-plunge type structure is that there is no need for deaeration before the tunnel. This is because the velocity with which the jets plunge onto each baffle is relatively low. In a comparable plunge-type shaft, the jet impingement velocity is considerably larger, leading to considerable air entrainment and the need for deaeration before the tunnel. Consequently, at larger drop heights, a plunge shaft may not be an attractive alternative. In comparison with a vortex shaft, the baffle-drop shaft stands out (1) by not requiring a specific approach channel design to precondition the inflow to the shaft and (2) by not requiring deaeration. One of the disadvantages of a baffle-drop structure is its size. Compared to a vortex shaft, its diameter is typically approximately five times larger. This fact may make the vortex drop structure more attractive at larger discharges and drop heights.

Acknowledgments

This paper is based in part on results of laboratory tests conducted at IIHR-Hydroscience and Engineering for the Regional Municipality of York, the Northeast Ohio Regional Sewer District, and the City of Indianapolis.

Notation

The following symbols are used in this paper:

A = adit inlet area;
B = baffle edge width (see Fig. 2);
C_d = discharge coefficient;
D = shaft diameter;
d = adit inlet diameter;
E = dry-space/access requirement (see Fig. 2);

F = baffle Froude Number = $[Q^2/(B^5 g)]^{1/3}$;
g = acceleration owing to gravity;
H = height of shaft-water surface elevation above adit-inlet invert;
h = baffle spacing (see Fig. 3);
h_v = venting allowance (see Fig. 3);
Q = design discharge;
t = baffle thickness (see Fig. 3);
y_c = critical depth on baffle shelf;
α = bulking factor; and
β = factor ≈ 0.55.

References

Ervine, D. A., and Kolkman, P. A. (1980). "Air entrainment and transport in closed conduit hydraulic structures." Delft Hydraulics Laboratory, Delft, Netherlands.

Falvey, H. T. (1980). "Air-water flow in hydraulic structures." *Engineering Monograph No. 41*, U.S. Dept. of the Interior, Water and Power Resources Services, Denver.

Jain, S. C. (1988). "Air transport in vortex-flow drop shafts." *J. Hydraul. Eng.*, 114(12), 1485–1497.

Jain, S. C., and Kennedy, J. F. (1983). "Vortex-flow drop structures for the Milwaukee Metropolitan Sewerage District inline storage system," *IIHR Rep. 264*, Univ. of Iowa, Iowa City, IA.

Lyons, T. C., and Odgaard, A. J. (2010). "Hydraulic model studies for the Regional Municipality of York Southeast collector drop structures." *IIHR LDR Rep. 365*, Univ. of Iowa, Iowa City, IA.

Lyons, T. C., Odgaard, A. J., and Craig, A. (2011). "Baffle drop structure design and hydraulic model studies for the City of Indianapolis Fall Creek/White River tunnel system." *IIHR LDR Rep. 372*, Univ. of Iowa, Iowa City, IA.

Lyons, T. C., Odgaard, A. J., and Jain, S. C. (2007). "Hydraulic model study for the Northeast Ohio Regional Sewer District Euclid Creek tunnel/baffle drop structure." *IIHR LDR Rep. 352*, Univ. of Iowa, Iowa City, IA.

Margevicius, A., Lyons, T., Schreiber, A., Switalski, R., Benton, S., and Glovick, S. (2009). "A baffling solution to a complex problem involving sewage drop structures." *Proc., 33rd IAHR Congress: Water Engineering for a Sustainable Environment*, IAHR, Madrid, Spain.

McKeogh, E. J., and Ervine, D. A. (1981). "Air entrainment rate and diffusion pattern of plunging liquid jets." *Chem. Eng. Sci.*, 36(7), 1161–1172.

U.S. Army Corps of Engineers. (1997). "Tunnels and shafts in rock." Chapter 6, *Engineer Manual EM 1110-2-2901*, Washington, DC.

Yu, D., and Lee, J. H. W. (2009). "Hydraulics of tangential vortex intake for urban drainage." *J. Hydraul. Eng.*, 135(3), 164–174.

J. Hydraul. Eng. 2013.139:995-1002.